AIAA JOURNAL
Vol. 35, No. 6, June 1997

Flight Effects on the Far-Field Noise of a Heated Supersonic Jet

A. Krothapalli,* P. T. Soderman,† C. S. Allen,‡ J. A. Hayes,§ and S. M. Jaeger‡
NASA Ames Research Center, Moffett Field, California 94035

The influence of forward flight on the far-field noise of an underexpanded heated supersonic jet has been studied experimentally with a 12.5-cm-diam convergent nozzle operated in the NASA Ames Research Center 12.2 × 24.4 m (40 × 80 ft) wind tunnel. The nozzle was operated at nozzle pressure ratios up to 4.5 and stagnation temperature ratios from 2.45 to 3.45. The resulting velocity (based on fully expanded condition) range is from 586 to 858 m/s. The freestream Mach number was varied from 0 to 0.32. Far-field narrow band spectra were obtained at angles (measured from the inlet axis) covering a range from 30 to 155 deg. A small amplification of the overall sound-pressure level (2 dB) due to forward flight is observed in the forward quadrant. The mixing noise reduction in the aft quadrant due to forward flight is much smaller than that observed in corresponding cold jets.

I. Introduction

SINCE the early work of Westley and Lilley[1] and of Lighthill,[2] the noise of jets has been a subject of extensive study. As a consequence, the noise generation mechanisms of subsonic jets, typified by the current high-bypass engines, are fairly well understood. However, with respect to supersonic jets, there is still a lack of knowledge about such basic matters as which region of the jet generates the most sound power. As such, very little progress has been made in development of an effective supersonic jet noise suppressor. The most recent attempt is the multilobe mixer/ejector noise suppressor that has its origins in the work of Westley and Lilley.[1] In light of this, a program of research is under way to shed further light on this problem with the hope of finding an engineering solution that can help the design of a better noise suppressor. In this paper, we describe the characteristics of the far-field noise of a supersonic jet that is operating at realistic engine operating conditions with simulated forward flight.

Our current understanding of the theory of supersonic jet noise is summarized in recent reviews by Tam.[3,4] In addition to the mixing noise, discrete and broadband shock-associated noise contributes significantly to the overall sound power of a supersonic jet. The characteristics of these different noise components and their dependence on various parameters were described by Tam, but because of the limited experimental data, much of this theory relied on the information of small-scale cold jets under static conditions. In fact, most previous investigations on supersonic jet noise are carried out with small-scale models at moderate Reynolds numbers and at low temperatures. In contrast, the current work presents far-field supersonic jet noise information of heated jets of larger scale and Reynolds number.

The far-field noise from high-temperature supersonic jets was studied by Tanna et al.[5] under static conditions. Recently, Seiner et al.[6] have conducted experiments to study the effects of temperature on an ideally expanded supersonic jet noise emission at an exit Mach number of 2. However, these tests provided no information concerning forward-flight effects. Norum and Shearin[7,8] investigated the effect of forward flight on aerodynamic and acoustic characteristics of an underexpanded cold (stagnation temperature is close to the ambient temperature) jet. To simulate the forward flight, a large-diameter secondary airflow was discharged around the jet into an anechoic chamber. The noise radiated from the primary supersonic jet therefore propagated across the entire secondary jet and across its mixing region toward the far-field microphones at rest in the ambient fluid. The measurements made under such simulated flight conditions are easy to obtain but difficult to translate into corresponding far-field data.

The acoustical complications of a free-jet facility are delineated by Morfey and Tester,[9] who developed facility-to-flight refraction corrections by using geometric acoustics and a straightforward Doppler frequency shift. Ahuja et al.[10] conducted a study of transmission, reflection, and scattering of sound in a free-jet shear layer with model noise sources where the angle changes associated with ray paths across the shear layer were determined. A later theoretical and experimental study by Schlinker and Amiet[11] suggested further corrections to such problems as partial reflection, spatial, and frequency scattering through the outer free-jet shear layer. Their analysis shows that scattering can become a problem when the ratio of the shear layer thickness to the wavelength of the sound is about 10 and higher. Thus, interpretation of the data at high frequencies can be quite difficult. In the present study, the far-field measurements were obtained with in-flow microphones, which reduced the uncertainty of the results.

Static and in-flight noise measurements of jet noise were also made with a unique facility,[12] known as the "aerotrain," to understand the effect of flight on jet noise. The aerotrain is an air cushion vehicle that moves along an inverted T track. A GE-J85 engine mounted on top of the vehicle served as the noise generator. Convergent and convergent–divergent nozzles were fitted to this engine. The engine was operated up to a nozzle pressure ratio of 2.4 and at a jet temperature of 1000 K. The effect of motion on the mixing noise has been clearly borne out from these measurements[13]; however, few data were gathered to provide an understanding of the flight effect on the shock-associated noise, an important component of the supersonic jet noise. The aerotrain data were also used by Michalke and Michel,[14] who derived an improved prediction formula for flight effects that takes into account jet temperature.

As opposed to free-jet wind tunnel or aerotrain simulations, a more satisfactory simulation of flight effects is done with inflow microphones in a wind tunnel having a closed test section that is designed to be anechoic in the desired frequency range and to have a low background noise level. Acoustic measurements in closed test section wind tunnels do have their inevitable shortcomings; however, none of these shortcomings is fundamental and they can be made insignificant by intelligent use of inflow microphones,[15,16] anechoic wind tunnel walls,[17] and microphone arrays.[18] Such is the case in the present experiment, except for the microphone array, as described in the next section.

Presented as Paper 96-1720 at the AIAA/CEAS 2nd Aeroacoustics Conference, State College, PA, May 6–8, 1996; received June 11, 1996; revision received Feb. 12, 1997; accepted for publication March 13, 1997.

*National Research Council Senior Research Fellow; currently Don Fuqua Professor and Chairman, Department of Mechanical Engineering, 2525 Pottsdamer Street, Florida A&M University and Florida State University, Tallahassee, FL 32310. Associate Fellow AIAA.

†Aeroacoustics Group Leader, Low Speed Aerodynamics Branch. Associate Fellow AIAA.

‡Aerospace Engineer, Sterling Federal Systems. Member AIAA.

§Aerospace Engineer, Low Speed Aerodynamics Branch. Member AIAA.

The far-field acoustic data of the present study are presented for a jet issuing from an axisymmetric convergent nozzle at high temperatures and in the presence of freestream velocity. The nozzle used was considerably larger than those used previously, thus providing an opportunity to obtain data at high Reynolds numbers, which can be extended easily to full-scale nozzle acoustics. In particular, the effect of forward flight on the supersonic jet noise is explored with these data.

II. Apparatus and Procedures

The experimental data were obtained from an investigation of the far-field noise generated by an underexpanded jet issuing from a convergent long-radius American Society of Mechanical Engineers (ASME) nozzle (see Fig. 1). The nozzle exit diameter D was 12.54 cm (4.937 in.). The test conditions are given in Table 1, where the Reynolds number is based on the nozzle exit conditions. The experiment was conducted in the national full-scale aerodynamics complex 40 × 80 ft wind tunnel test section, which is known to be sufficiently anechoic to 500 Hz. For forward-flight effects, the freestream Mach number was fixed at 0.12, 0.24, and 0.32. The nozzle and its mounting arrangement in the test section are shown in Fig. 2.

The far-field noise directivity was obtained with B&K 4135, 6.35-mm (0.25 in.) diameter condenser microphones with the flow-induced tone eliminator (FITE) aerodynamic microphone forebody (AMF).[15] Figure 3 shows the FITE, which incorporates a B&K type UA 0385 nose cone screen and cavity. There are two interrelated effects of using this type of protective device. First, the AMF along with the screen and cavity, sometimes called a nose cone, modifies the acoustic field and the microphone's response as a function of frequency and incident angle. Second, the use of an AMF for inflow measurements requires the microphone to be pointed streamwise into the flow instead of at the source, creating a nonzero acoustic incidence angle. Corrections that account for these effects were developed in a representative acoustic field with microphones in the bare and AMF-covered configurations. The two configurations can then be related to determine the AMF effect. This relationship is

Table 1 Jet conditions

NPR	T_0, K	U_j, m/s	M_j	$Re \times 10^6$
2.5	737	586	1.24	1.1
3.0	824	670	1.37	0.9
3.4	883	727	1.46	0.8
4.0	971	803	1.58	0.7
4.5	1033	858	1.66	0.6

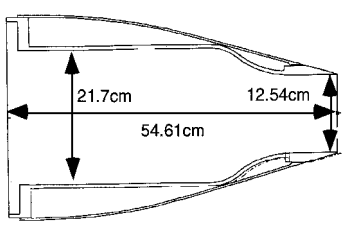

Fig. 1 Schematic of the nozzle geometry.

Fig. 2 Photograph of the model in the 40 × 80 ft wind tunnel.

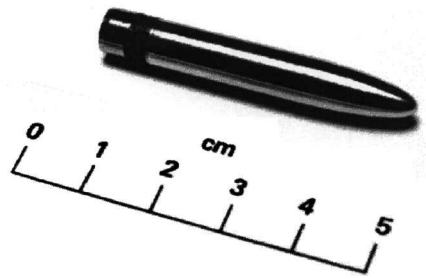

Fig. 3 Picture of the microphone forebody.

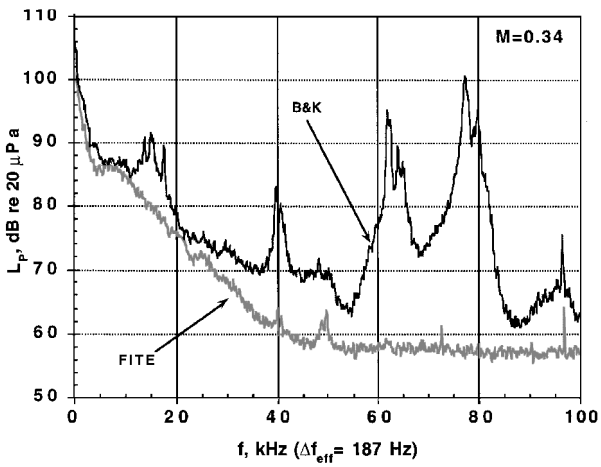

Fig. 4 Comparison of the spectra taken with the standard B&K microphone forebody and the FITE aerodynamic microphone forebody.

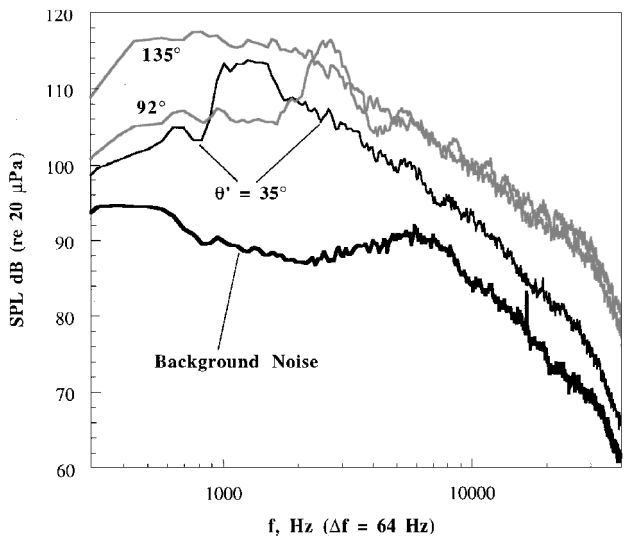

Fig. 5 Comparison of the background noise spectra of the tunnel with the jet noise: NPR = 3.4, temperature ratio = 3.0, and M_∞ = 0.32.

calculated by estimating the magnitude of the frequency response or transfer function, called the "gain factor," between the bare and the AMF-covered configurations. The resulting transfer function magnitudes are then applied to the test data together with the other microphone corrections.[16] The flow noise reduction obtained with the FITE AMF compared to the standard B&K nose cone is shown in Fig. 4. The data clearly suggest that a significant background noise reduction is obtained with the FITE microphone forebody, especially at high frequencies. High-amplitude tones that are commonly observed in spectra with standard nose cones are nearly eliminated. Figure 5 shows a comparison between the test section background noise and the jet noise at M_∞ = 0.32. The background data measurement had an uncertainty of about 1 dB. To achieve a measurement accuracy of about 0.5 dB, the background noise must be at least 6 dB below the signal level.[16] For most of the test conditions, such a

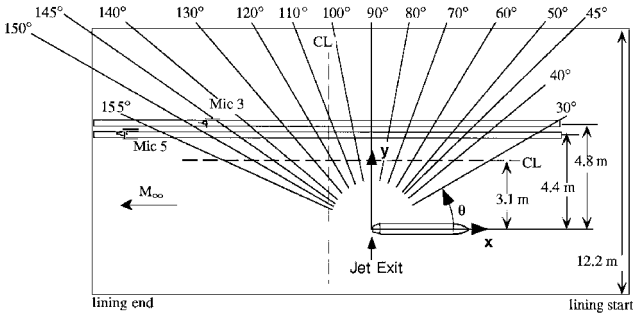

Fig. 6 Schematic of the microphone traverse locations.

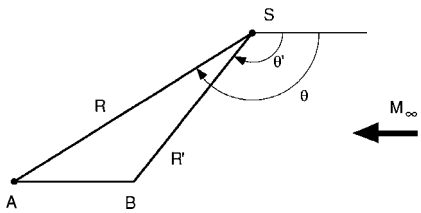

Fig. 7 Schematic of the forward-flight effect on the emission angle.

criterion was met in the present experiment. A detailed description of the background noise in the tunnel section is given by Jaeger et al.[17]

The narrow-band (frequency resolution = 64 Hz) frequency spectra covering a range from 0 to 70 KHz were obtained with an estimated accuracy of $\pm$0.6 dB. Microphones were mounted on single-axis traverses, which were located 4.39 m (35D) and 4.8 m (38.2D) from the jet axis (see Fig. 6). The data are extrapolated to a far-field circular arc of radius 100D by removing the atmospheric absorption and taking into account spherical spreading. The data are presented in terms of the angle to the inlet centerline axis. To ensure that both geometric and acoustic far-field conditions exist, it is desirable to make noise measurements at a distance in excess of 100D from the nozzle exit. For the Strouhal number range considered in this experiment, the far-field condition, as typically characterized by the inverse-square-law variation of the mean square pressure with distance, is believed to be met at 35D in accordance with the investigations of Ahuja et al.[19]

The forward-flight data also require consideration of wind velocity on the fixed microphone results. The data were taken at fixed angles, θ. However, to compare data at different freestream velocities, it is necessary to compare the data for a given emission angle θ'. Using the simple schematic shown in the Fig. 7, a formula can be derived to account for the convection effect. Consider a fixed source S and a fixed microphone A immersed in a freestream that is moving at Mach number M_∞. The sound waves would have propagated along vector $\boldsymbol{R}'$ in still air with an emission angle θ' but in wind are convected along the path $\boldsymbol{R}$ to the microphone in the direction θ. From geometry, it can be shown that the data measured in forward flight at microphone angle θ are related to the emission angle θ' by the following formula:

$$\theta' = \cos^{-1}\left(M_\infty \sin^2\theta + \cos\theta\sqrt{1 - M_\infty^2 \sin^2\theta}\right)$$

Throughout this paper, the emission angle θ' is used when considering the forward-flight data (note that $\theta = \theta'$ for $M_\infty = 0$).

III. Results and Discussion

Typical narrow-band spectra representing far-field noise are shown in Fig. 8. The three dominant components of the noise, i.e., the screech tone, broadband shock-associated noise, and the mixing noise, are clearly identified (indicated by letters a, b, and c, respectively) in the spectra of the top plot of Fig. 8. The discrete component of the noise, referred to as screech tone, is identified by its invariance with the angle of observation. The shock-associated noise is identified by a spectral peak with relatively narrow bandwidth. The frequency of the spectral peak is a function of the direction of radiation with a lowest value near the jet inlet direction and increases monotonically in the jet flow direction. The turbulent mixing noise

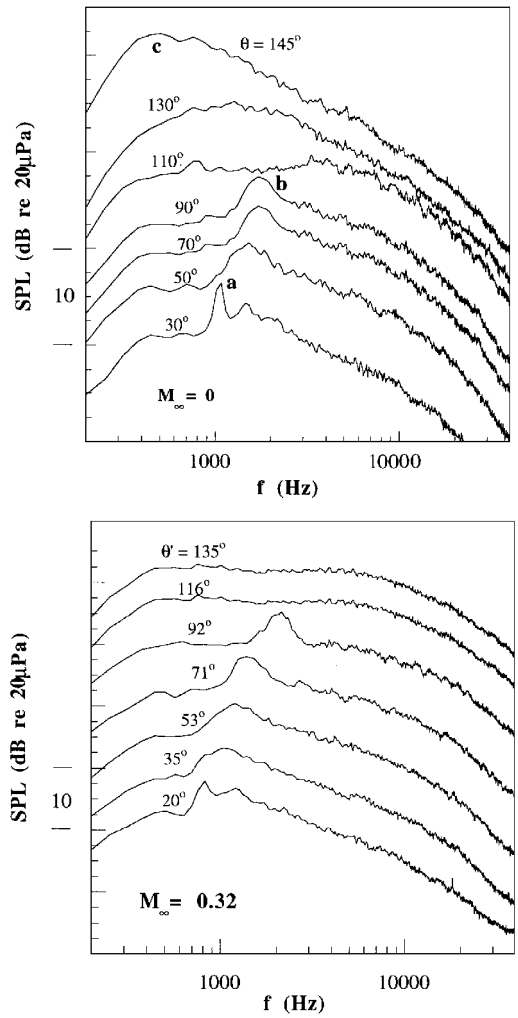

Fig. 8 Narrow-band far-field (100D) spectra with and without forward-flight effect: NPR = 4.5 and temperature ratio = 3.45: a, screech tone; b, broadband shock-associated noise; and c, mixing noise.

is typically identified with a broad peak in the spectra that is most dominant in the aft quadrant. The corresponding spectra in the bottom plot of Fig. 8 are shown to elucidate the effects of the forward flight. These effects on each of the components of the noise are discussed below. Because the jet produces noise from different types of sources, it is convenient to treat these three components separately. However, contributions to the frequency spectra at a given angle may come from all three components of the jet noise. The discussion is based on selected data, but the conclusions are generally supported by the data taken at all of the operating conditions listed in Table 1.

A. Screech Tone

The screech tone is identified with a sharp spike in the spectrum denoted in Fig. 8 by the letter a. At 30 deg, the amplitude of the screech tone is less than the normally observed amplitude for cold jets operating at the same nozzle-pressure ratio (NPR). Under static conditions, the details of the screech frequency and amplitude variations with nozzle pressure and temperature ratios were discussed recently by Krothapalli and Strykowski.[20] Unlike cold jets, where the screech tone is accompanied by its harmonics, only the tone at its fundamental frequency is observed here. Very little energy in the spectral peak associated with the screech tone is found at angles greater than about 70 deg.

Tam[3] developed a prediction formula for the screech frequency as follows:

$$\frac{f_s D_j}{U_j} = \frac{0.67}{(M_j^2 - 1)^{\frac{1}{2}}}\left(1 + \frac{0.7 M_j}{\left\{1 + [(\gamma - 1)/2] M_j^2\right\}^{\frac{1}{2}}}\left(\frac{T_0}{T_a}\right)^{\frac{1}{2}}\right)^{-1}$$

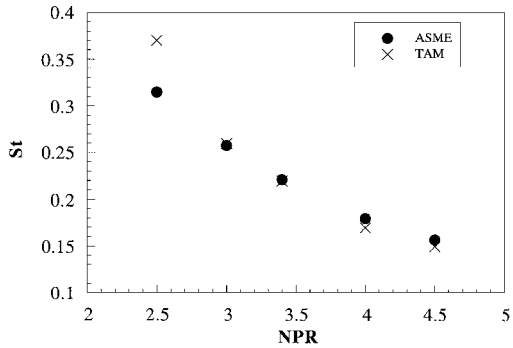

Fig. 9 Variation of the screech frequency with NPR at high temperature ratios (2.5–3.5).

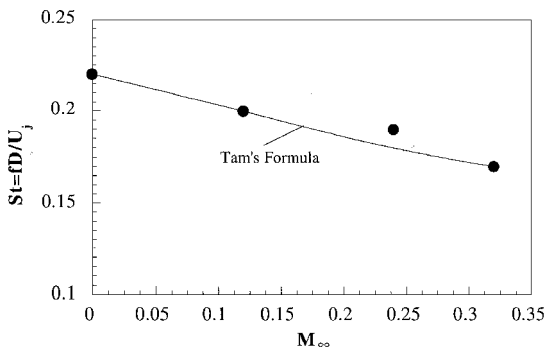

Fig. 10 Variation of screech Strouhal number with the forward-flight Mach number.

where the fully expanded jet diameter D_j is obtained by imposing the condition of conservation of mass flux and is related to D by

$$\frac{D_j}{D} = \left\{\frac{1+[(\gamma-1)/2]M_j^2}{1+[(\gamma-1)/2]M_d^2}\right\}^{(\gamma+1)/4(\gamma-1)} \left(\frac{M_d}{M_j}\right)^{\frac{1}{2}}$$

M_j and M_d are fully expanded jet Mach number and the nozzle design Mach number for wave-free operation, respectively. In the present experiment, $M_d = 1$. Figure 9 shows a comparison of the data with that of the prediction. The constant 0.67 in the equation has been replaced with 0.62 for better agreement. The actual value of this constant, which is proportional to the shock cell spacing, may need further examination. The formula overpredicts the screech frequency at lower NPR. It is believed that the nozzle at this NPR is operating in a different mode than that assumed in Tam's analysis. Tam's formula was derived by taking into account only the helical mode that is dominant in hot jets.

The effect of the forward flight on the screech tone is shown in Fig. 10. The particular angle $\theta\prime = 30$ deg was chosen because the dominant direction of radiation of the screech tone falls within the forward arc. The Strouhal number corresponding to screech frequency decreases with forward-flight Mach number in accordance with the formula (similar to the one shown earlier) developed by Tam,[3] shown by the solid line in Fig. 10. The closed symbols represent the data. The effect of the forward flight on the amplitude of the screech tone is shown in Fig. 11. It is evident that the intensity of the screech tone is unaffected by the forward flight. However, there is an increase in amplitude of the spectrum with forward flight in the frequency range of dominant shock-associated noise. The effects of flight on the broadband shock-associated noise are discussed in the next section.

Intense screech tones were observed by Norum and Shearin[8] with cold jets in forward flight. Their spectra are dominated by several peaks that correspond to the screech tone and its harmonics, and they appear in all of the spectra covering a range of $\theta = 40$–150 deg. In high-temperature jets, very little energy is contained in the harmonics. In addition, these screech tones themselves are confined to a small region in the forward arc as shown in Fig. 8. These results show that, at elevated jet temperatures, the screech tones contribute

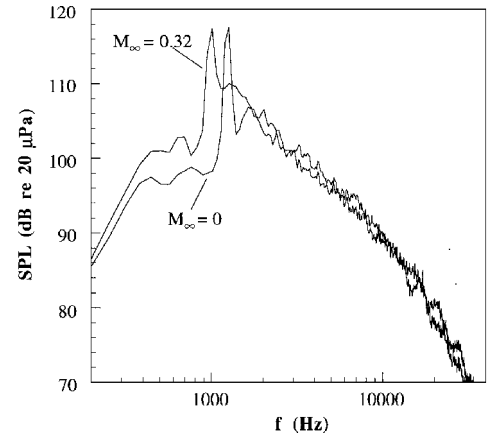

Fig. 11 Far-field spectra with and without forward flight in the forward arc: NPR = 3.4, temperature ratio = 3.0, and $\theta\prime = 30$ deg.

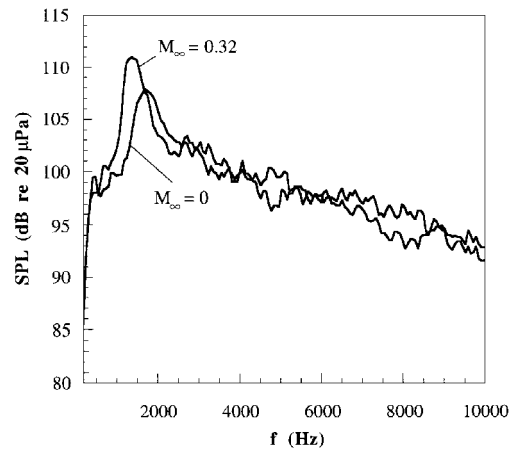

Fig. 12 Far-field spectra representing the broadband shock-associated noise: NPR = 4.5, temperature ratio = 3.45, and $\theta\prime = 70$ deg.

little to the overall far-field noise. As the jet temperature is increased, three-dimensional instability wave-amplification rates significantly exceed their two-dimensional counterpart because of increased convective Mach number (for more details, see Ref. 20). This results in a loss of axisymmetric coherence in the flow, which in turn weakens the feedback loop, thereby reducing the screech amplitude.

B. Broadband Shock-Associated Noise

The broadband spectral peak dominant in the region of $50 < \theta\prime < 110$ deg and labeled b in Fig. 8 represents the broadband shock-associated noise. Unlike the screech tone, its peak frequency is a function of the direction of radiation with the lowest frequency being near the jet inlet direction ($\theta\prime = 0$ deg). Similar to the screech tone, its peak frequency decreases with the forward flight as shown in Fig. 12. In addition, the spectral peak becomes narrower with the forward velocity. Considering the spectral characteristics, these observations are similar to those made by Norum and Shearin.[8] The broadband shock-associated noise is generated by the interaction of the instability waves in the shear layer of the jet and the quasi-periodic shock cell structure. The presence of uniform velocity will modify the shock-cell spacing and the characteristics of the instability waves. Taking into account these modifications, Tam[21] developed a theoretical model that predicts the spectral characteristics, such as peak frequency and half-width reduction, with reasonable accuracy. However, the peak amplitude increase due to forward flight shown in Fig. 12 is difficult to deduce from this theory.

Typically, an increase in the spectral peak associated with the broadband shock-associated noise is attributed to the convective amplification of the sources. However, the nature of these noise sources is not clearly known, making it difficult to employ the convective amplification factors derived with simple sources, such as the one developed by Dowling.[22] More work is needed to isolate

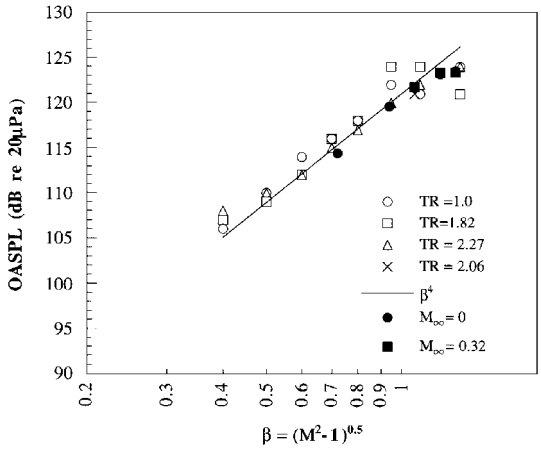

Fig. 13 Variation of the OASPL with the shock parameter at $\theta\prime = 90$ deg. Open symbols represent data from Ref. 5.

the forward-flight effects on the noise source modification and the mean flow convection. However, the 2-dB reduction seen at 70 deg can be accounted for by applying the fourth power of the Doppler factor $[(1 - M_j \cos\theta)^4]$.

The intensity of broadband shock-associated noise is primarily a function of the nozzle pressure ratio and largely independent of the temperature ratio. For a given radiation direction, the measured overall sound pressure level (OASPL) has been observed to scale well with a parameter β, where $\beta = \sqrt{(M_j^2 - 1)}$ is related to the fully expanded jet Mach number M_j, as shown in Fig. 13 at $\theta\prime = 90$ deg. The data from Ref. 5 are included for comparison with the present data. When plotted in this fashion, the OASPL varies as β^4, as shown, which is in accord with theoretical arguments proposed by Harper-Bourne and Fisher.[23] The noise radiation at 90 deg in forward flight also follows the β^4 variation, as shown. The parameter β characterizes the pressure jump across a normal shock at Mach number M_j. Because the forward-flight velocity does not change the pressure variations within the shock-cell structure, the agreement of the forward-flight data at $\theta\prime = 90$ deg with the corresponding static jet is anticipated. At large NPR, the data begin to deviate from this law because of the presence of a Mach disk, which significantly alters the shock-cell structure. The data for static- and forward-flight conditions are almost identical at high β values. In cold jets, the shock-associated noise dominates over the turbulent mixing noise except in the aft quadrant. At elevated jet temperatures, the turbulent mixing noise contribution increases, and the shock-associated noise remains unchanged. At the jet temperatures considered here, the mixing noise dominates in the aft region starting at $\theta\prime = 110$ deg (see Fig. 8).

C. Mixing Noise

The spectral characteristics of the flight effect on mixing noise are illustrated in Fig. 14. These spectra were taken at large angles to the inlet axis (i.e., aft quadrant) for two different jet operating conditions. One of the distinct characteristics of the mixing noise is that it is highly directional with a broad low-frequency peak in the spectra. The mixing noise generation process is closely linked to the characteristics of large-scale instability waves of the jet.[3,23] As is generally expected, the presence of the uniform stream in forward flight causes the mixing region close to the nozzle exit to be altered with reduced shear, thereby changing the instability process that results in reduced far-field noise. At moderately underexpanded conditions (NPR = 3.4), the reduction in noise occurs at all frequencies, with maximum effect found at low frequencies as shown in Fig. 14a. The reduction found at low frequencies may also be due to lesser shock-associated noise in the aft quadrant in the presence of forward flight. However, at higher temperatures and NPR, the favorable effect of flight begins to diminish, especially at high frequencies, as shown in Fig. 14b. These observations are consistent with many previous experimental results, as discussed by Michalke and Michel.[14]

In Fig. 15, the static and forward-flight OASPL directivities are compared at a NPR of 3.4. The data clearly show that the noise is

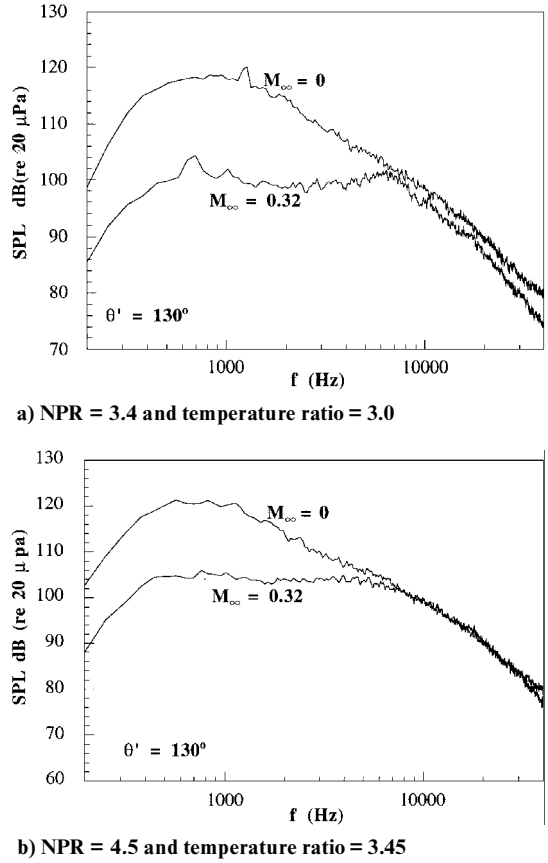

a) NPR = 3.4 and temperature ratio = 3.0

b) NPR = 4.5 and temperature ratio = 3.45

Fig. 14 Far-field spectra in the aft quadrant representing the dominant mixing noise.

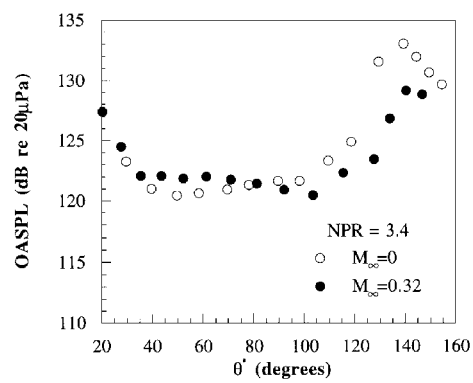

Fig. 15 Comparison of the static and forward-flight far-field directivity at NPR = 3.4 and temperature ratio = 3.0.

significantly reduced by flight in the aft quadrant. This reduction gets smaller when the angle is decreased. In the forward quadrant, a slight increase ($\approx$2 dB) in the intensity is observed. The changes in magnitude of the OASPL are shown in Fig. 16 as ΔOASPL. With increasing pressure and temperature ratios, the reduction in the mixing noise with flight is not as significant. Aerotrain results taken at low-pressure ratios[13] (where shock-associated noise is quite minimal) and predictions of Michalke and Michel[14] indicate a much larger ($\approx$10 dB) decrease in the mixing noise with forward flight. The lack of significant noise reduction in the aft quadrant and less than normal amplification in the forward arc cannot be explained satisfactorily by any of the existing theories.

Unfortunately, prediction formulas used to account for forward flight are based on high-frequency approximations and compact noise source models. Typical sources in jets under consideration here are noncompact and statistically random in nature. Prediction models that take into account realistic source properties were developed by Tam[24] for broadband shock-associated noise with some success. However, similar models for mixing noise are yet to be developed.

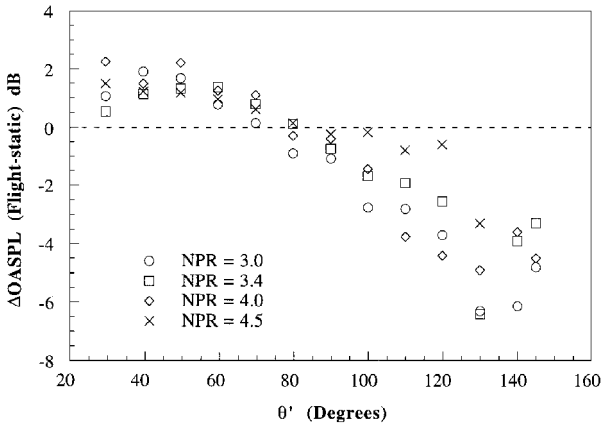

Fig. 16 Net change in the OASPL directivity with forward flight.

IV. Conclusions

The influence of forward flight on the noise generated by an underexpanded axisymmetric jet has been studied over a range of engine operating parameters. These measurements were taken in a large wind tunnel under anechoic and low background noise conditions. To compare with the static data, appropriate corrections to account for inflow microphone measurements and convection are made.

The three distinct noise sources are apparent in the far-field spectra: screech tones, broadband shock-associated noise, and mixing noise. Screech tones are confined only to a small region in the forward arc and very little energy is found in the harmonics. The variation of screech frequency with forward flight is in accord with the prediction formula proposed by Tam.[3]

The spectral peak corresponding to the broadband shock-associated noise decreases in frequency with increased forward flight. The overall sound pressure level at 90 deg to the jet axis follows a commonly known β^4 law and is not affected by forward flight.

From the directivity measurements, a small increase (2 dB) in the OASPL of the forward arc, reflecting an increase in the broadband shock-associated noise, is observed. Previous theoretical studies indicate a much larger increase because of convective amplification that is not supported by the present experimental results.

A noticeable decrease in the mixing noise in the aft quadrant is observed in the presence of forward flight. However, with increasing pressure ratio, the magnitude of this decrease appears to diminish.

Acknowledgments

The first author would like to thank the National Research Council for its support of his stay at the NASA Ames Research Center. The continuing research support of NASA Headquarters, under Grant NAG 2930, is also appreciated.

References

[1]Westley, R., and Lilley, G. M., "An Investigation of the Noise Field from a Small Jet and Methods for its Reduction," College of Aeronautics, Rept. 53, Cranfield, England, UK, 1952.

[2]Lighthill, M. J., "On Sound Generated Aerodynamically, I. General Theory," *Proceedings of the Royal Society of London, Series A: Mathematical and Physical Sciences*, Vol. 211, No. 1107, 1952, p. 564.

[3]Tam, C. K. W., "Jet Noise Generated by Large-Scale Coherent Motion," Aeroacoustics of Flight Vehicles: Theory and Practice, NASA RP 1258, Vol. 1, 1991, p. 311.

[4]Tam, C. K. W., "Supersonic Jet Noise," *Annual Review of Fluid Mechanics*, Vol. 27, 1995, p. 17.

[5]Tanna, H. K., Dean, P. D., and Burrin, R. H., "The Generation and Radiation of Supersonic Jet Noise," Vol. 4: Shock-Associated Noise Data, AFAPL TR-76-65, 1976.

[6]Seiner, J. M., Ponton, M. K., Jansen, B. J., and Lagen, N. T., "The Effects of Temperature on Supersonic Jet Noise Emission," *Proceedings of DGLR/AIAA 14th Aeroacoustics Conference*, AIAA, Washington, DC, 1992 (DGLR-Bericht 92-03).

[7]Norum, T. D., and Shearin, J. G., "Effects of Simulated Flight on the Structure and Noise of Underexpanded Jets," NASA TP 2308, 1984.

[8]Norum, T. D., and Shearin, J. G., "Shock Structure and Noise of Supersonic Jets in Simulated Flight to Mach 0.4," NASA TP 2785, 1988.

[9]Morfey, C. L., and Tester, B. J., "Noise Measurements in a Free Jet Flight Simulation Facility: Shear Layer Refraction and Facility-to-Flight Corrections," *Journal of Sound and Vibration*, Vol. 54, No. 1, 1977, pp. 83–106.

[10]Ahuja, K. K., Tanna, H. K., and Tester, B. J., "An Experimental Study of Transmission, Reflection and Scattering of Sound in a Free Jet Flight Simulation Facility and Comparison with Theory," *Journal of Sound and Vibration*, Vol. 75, No. 1, 1981, pp. 51–85.

[11]Schlinker, R. H., and Amiet, R. K., "Shear Layer Refraction and Scattering of Sound," *Sixth Aeroacoustics Conference*, AIAA, Washington, DC, 1980 (Paper 80-0973).

[12]Hoch, R. G., and Berthelot, M., "Use of the Bertin Aerotrain for the Investigation of Flight Effects on Aircraft Engine Exhaust Noise," *Journal of Sound and Vibration*, Vol. 54, No. 2, 1977, pp. 153–172.

[13]Drevet, P., Duponchel, J. P., and Jacques, J. R., "The Effect of Flight on Jet Noise as Observed on the Bertin Aerotrain," *Journal of Sound and Vibration*, Vol. 54, No. 2, 1977, pp 173–201.

[14]Michalke, A., and Michel, U., "Prediction of Jet Noise in Flight from Static Tests," *Journal of Sound and Vibration*, Vol. 67, No. 3, 1979, p. 341.

[15]Allen, C. S., and Soderman, P. T., "Aeroacoustic Probe Design for Microphone to Reduce Flow-Induced Self-Noise," AIAA Paper 93-4343, Oct. 1993.

[16]Allen, C. S., Vandra, K., and Soderman, P. T., "Microphone Corrections for Accurate In-flow Acoustic Measurements at High Frequency," CEAS/AIAA Paper 95-150, June 1995.

[17]Jaeger, S. M., Allen, C. S., and Soderman, P. T., "Reduction of Background Noise in the NASA Ames 40-by-80 Foot Wind Tunnel," CEAS/AIAA Paper 95-152, June 1995.

[18]Mosher, M., "Phase Arrays for Aeroacoustic Testing: Theoretical Development," *Proceedings of the AIAA/CEAS 2nd Aeroacoustics Conference*, AIAA, Washington, DC, 1996 (Paper 96-1713).

[19]Ahuja, K. K., Tester, B. J., and Tanna, H. K., "Calculation of Far-Field Jet Noise Spectrum from Near-Field Measurements Using True Source Location," *AIAA 11th Fluid and Plasma Dynamics Conference*, AIAA, Washington, DC, 1978 (Paper 78-1153).

[20]Krothapalli, A., and Strykowski, P. J., "Revisiting Screech Tones: Effects of Temperature," AIAA Paper 96-0644, Jan. 1996.

[21]Tam, C. K. W., "Broadband Shock-Associated Noise From Supersonic Jets in Flight," *Journal of Sound and Vibration*, Vol. 151, No. 1, 1991, p. 131.

[22]Dowling, A., "Convective Amplification of Real Simple Sources," *Journal of Fluid Mechanics*, Vol. 74, Pt. 3, 1976, p. 529.

[23]Harper-Bourne, M., and Fisher, M. J., "The Noise from Shock Waves in Supersonic Jets," Noise Mechanisms, AGARD CP-131, March 1974, p. 11-1.

[24]Tam, C. K. W., "Broadband Shock Associated Noise from Supersonic Jets Measured by a Ground Observer," *AIAA Journal*, Vol. 30, No. 10, 1992, p. 2395.

S. Glegg
Associate Editor